ROMANIAN ACADEMY
"PETRU PONI"
Institute of Macromolecular Chemistry

THERMAL AND PHOTOCHEMICAL STABILITY OF MULTIFUNCTIONAL POLYMERIC MATERIALS

- Ph.D. thesis overview -

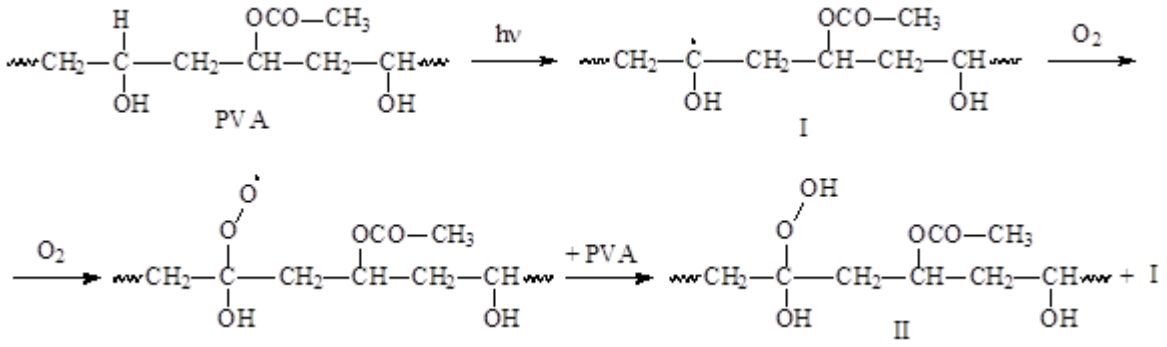

Scientific Supervisor
Acad. BOGDAN C. SIMIONESCU

Ph.D. Student
CRISTIAN–DRAGOȘ VARGANICI

Iassy – 2014

ROMANIAN ACADEMY
"PETRU PONI"
Institute of Macromolecular Chemistry

No 4506/ IX 2014

To Mrs./Mr._____

We hereby announce that on **October 27th, 2014**, at **12** o'clock, in the library of the "Petru Poni" Institute of Macromolecular Chemistry in Iassy, there will be held the public presentation of the Ph.D. thesis entitled "**THERMAL AND PHOTOCHEMICAL STABILITY OF MULTIFUNCTIONAL POLYMERIC MATERIALS**", elaborated by chemical engineer **Cristian–Dragoş Varganici**, in fulfillment of the requirements for the degree of Doctor of Phylosophy.

The doctoral committee is comprised of the following members:

PRESIDENT: **Dr. Valeria Harabagiu,** Scientific Researcher, qualification level I
"Petru Poni" Institute of Macromolecular Chemistry of Iassy

SCIENTIFIC SUPERVISOR: **Acad. Bogdan C. Simionescu**
"Petru Poni" Institute of Macromolecular Chemistry of Iassy

COMMITTEE: **Associate Prof. Dr. Eng. Constanţa Ibănescu**
Technical University "Gheorghe Asachi" of Iassy,
Faculty of Chemical Engineering and Environmental Protection

Prof. Dr. Mircea Palamaru
"Alexandru Ioan Cuza" University of Iassy, Faculty of Chemistry

Dr. Dan Roşu, Scientific Researcher, qualification level II
"Petru Poni" Institute of Macromolecular Chemistry of Iassy

In conformity with the Regulations regarding the organising and course of the doctorate for graduation in the Romanian Academy, we hereby send you the overview of the Ph.D. thesis with the kind request to send us your written appreciations and observations.

With this occasion we invite you to participate at the public presentation of the Ph.D. thesis.

DIRECTOR,

Dr. Anton Airinei

ACADEMIA ROMÂNĂ INSTITUTUL DE CHIMIE MACROMOLECULARĂ "PETRU PONI" IAŞI

ACKNOWLEDGEMENTS

The scientific fundamentation and elaboration of this Ph.D. thesis would have been impossible without the support, help, advice and coordination of some special persons which, by highly professional degree and passion, have contributed twoards my professional growth as a future researcher.

To Acad. Bogdan C. Simionescu (scientific supervisor),

Profound gratitude and appreciation for the trust, the scientific coordination, patience, highly professional degree, support and understanding showed throghout the entire doctoral studies period, thus contributing twoards my professional and personal formation.

To Mrs. Dr. Eng. Mariana Pinteală, Scientific Researcher, qualification level I,

All my gratitude, profound respect and appreciation for the support, help, advice, ideas, trust and patience generously offered throughout the entire period of scientific research included in the doctoral studies, thus contributing twoards my personal and professional growth. I would also like to thank Dr. Pinteală for her characteristic kindhearted nature.

To Mr. Dr. Dan Roșu, Scientific Researcher, qualification level II

and Mrs. Dr. Liliana Roșu, Scientific Researcher, qualification level III,

All my consideration, appreciation and gratitude for the constant support, understanding, trust and advice throughout the entire Ph.D. period. I would also like to thank them for the open and sincere collaboration and for their effort during the scientific research period for finalizing this Ph.D. thesis, thus contributing twoards my professional and personal evolution.

Great appreciation for all my ***colleagues of the Centre of Advanced Research for Bionanoconjugates and Biopolymers (IntelCentre)*** *for the professional and moral support during the Ph.D. years.*

Profound gratitude and appreciation to ***all research teams*** *whom I had the pleasure of collaborating with.*

Great appreciation for all ***colleagues of the „Petru Poni" Institute of Macromolecular Chemistry*** *for their support in characterization of compounds.*

I thank the ***Romanian Academy*** *for the financial support throughout the entire doctoral studies period (2011–2014).*

Last, but not least, I would like to thank ***my family*** *for their unconditional love, constant moral and financial support, understanding and encouragement throughout all these years.*

To my mother and sister...

Contents

USED ABBREVIATIONS

TGA – dynamic thermogravimetry

α – conversion degree

T – temperature

E_a – activation energy

β – heating rate

OFW – Flynn–Wall–Ozawa

DSC – differential scanning calorimetry

DTA – differential thermal analysis

rDA – retro-Diels–Alder

DTG – first derivative curve of mass loss in thermogravimetric analysis

FTIR – Fourier transform infrared spectroscopy

MS – mass spectrometry

PAV – poly(vinyl alcohol)

^{1}H–NMR – nuclear magnetic resonance spectroscopy

ESI–MS – electrospray interface mass spectrometry

DA – Diels–Alder

ATR – total attenuated reflectance

T_g – glass transition temperature

IPN – interpenetrating network

SIPN – semi–interpenetrating network

PUR – polyurethane

CER – crosslinked epoxy resin network

SEM – scanning electron microscopy

XPS – X–ray photoelectron spectroscopy

UV–Vis – UV–Visible spectroscopy

INTRODUCTION

During their lifetime all polymer based materials are exposed repeatedly or occasionally to the action of a series of distructive environmental factors such as light, humidity, temperature, UV radiations and oxygen. These factors may act individually or simultaneously and generate gradual and irreversible structural modifications in materials. The implications of such modifications lead to performance reduction of polymeric materials even towards the point of their disposal. Polymer based materials may be used either as individual products or component parts of some devices exposed unprotected in the environment. Regardless of the situation, polymeric materials undergo distructive processes in time. Due to this aspect, accumulation of knowledge on kinetic aspects and different mechanisms of decomposition reactions of polymers is highly sought in order to act efficiently in stabilization processes and correct evaluation of life–time prediction of materials. A deep knowledge of these aspects is also necesary for a correct planning of mentenance and its argumentation from the scientific point of view.

Polymers and polymer based materials may be used in different special applications, such as component parts of flying devices, construction materials for the electronic industries and automotive industry and other various types of equipment. Due to this aspect, the thermal stability of polymers and polymer based materials, amongst other physical and chemical properties, represents a key factor which must be tested and, where the case, improved. Thermal stability studies present great importance from an ecological point of view also, due to the hazardous environmental impact of the evolved gaseous products during thermal decomposition of polymers. A great deal of research is nowadays invested in technologies for recovery of polymers and corresponding monomers from polymer containing waste, thus advanced knowledge of different thermal decomposition mechanisms of polymers must be accumulated.

Due to the above mentioned aspects, in this Ph.D. thesis the following purposes are established:

I. Determination of the thermal stability of some natural and synthetic polymeric materials, studied under dynamic conditions and in inert atmosphere. The following criteria will be met:

- Determination of thermokinetic parameters values of thermal decomposition processes as recomended by the International Confederation for Thermal Analysis and Calorimetry (ICTAC);
- evolved gas analyses during thermal decomposition;
- elucidation of different thermal decomposition mechanisms.

II. Photochemical stability studies of polymer based materials. The following criteria will be met:

- influence of irradiation dose on the photostability in controlled conditions;
- investigation of surface properties modifications (gloss, color, roughness, contact angle) which occur during photochemical decomposition;
- investigation of properties modification during photodecomposition (mass loss, swelling degree);
- study of structural modifications resulted after photodecomposition process;
- establishment of photodecomposition mechanisms.

The Ph.D. thesis is structured in two parts comprising six chapters. The first part represents a literature study on theoretical aspects of thermal and photochemical stability of polymeric materials, while the second part presents the author's original contributions to these two research domains.

The Ph.D. thesis expands on **127** pages and contains a total of **18** tables, **48** figures, **16** schemes and **140** references.

Chapter I encompasses literature studies on theoretical aspects regarding kinetics of thermal decomposition processes and evaluation of present research in the field of thermal stability of polymeric materials.

Chapter II describes a summary of theoretical aspects regarding the diverse fotodegradation mechanisms of polymers and polymer based materials.

Chapter III presents the author's original contributions and is comprised of miscibility, thermal and photochemical behavior studies of some semi–interpenetrating polymer networks based on aromatic polyurethane and crosslinked epoxy resin.

Chapter IV shows author's original contributions regarding the establishment of a photodecomposition mechanism of some cryogels based on poly(vinyl alcohol) and cellulose.

Chpater V represents the detailed experimental methodology and characterization methods used in the author's studies.

The Ph.D. thesis ends with the general conclusions section (**Chapter VI**) and reference list.

The Ph.D. thesis overview presents the summary of the original contributions (Chapters III and IV) with respect to original chapter titles and tables, figures, schemes and references numbering.

ORIGINAL CONTRIBUTIONS

SEMI–INTERPENETRATING POLYMER NETWORKS BASED ON AROMATIC LINEAR POLYURETHANE AND EPOXY RESIN

Disadvantages such as brittleness, easy stress cracking under impact and stress after curing, limit the epoxy resins further applications in high–tech fields. Therefore much attention is paid to improve these properties. A way to improve the physico–mechanical properties of epoxy resins is by mixing them with elastomers.

Linear polyurethanes possess excellent elasticity, damping properties and abrasive resistance, yet they have no great resistance to humidity and temperature. In order to improve some properties of epoxy resins and linear polyurethanes, one method consists of the obtaining of interpenetrating polymer networks (IPN) and semi–interpentrating polymer networks (SIPN).

When a polymer with linear structure is entangled at molecular scale in the network of another polymer with cross–linked structure a semi–interpenetrating polymer network is formed. Epoxies and polyurethanes provide better overall combinations of film properties than any other organic coatings and are applied for protection of masonry and/or concrete constructions because the linear polyurethanes have excellent elasticity, abrasive resistance and damping properties and the epoxy resin networks are characterized by good adhesion to metals and high mechanical strength.

Six SIPNs based on aromatic linear polyurethane (PUR) and increasing concentrations of cross–linked epoxy resin network (CER) (5%, 10%, 20%, 30% and 40%) were used in the miscibility, thermal and photochemical stability studies.

For the obtaining of the SIPNs, there was used a PUR comprised of 4,4'–diphenilmethane diisocyanate (MDI), poly(ethylene adipate)diol (PEA), with an average numerical molecular mass value of 2000, and butylene glycol (BG) as chain extender, molar ratio 1:5:6. The epoxy resin was a commercial product (Ropoxid 501) with an average numerical molecular mass value of 380 and an epoxy equivalent of 0.525 equiv/100 g and comprised of 4,4'–isopropylidenediphenol and epichlorohydrin. The SIPNs were prepared according to a sequential procedure by mixing the PUR with variable amounts of CER in presence of ethylenediamine, used as cross–linking agent (Scheme 1.3).

The SIPNs based on an aromatic PU and increasing CER concentration showed a good miscibility, up to a CER content of 30%, which was established by the presence of a single glass transition temperature domain (Tg). DSC measurements and microscopy studies ((scannind electrone microscopy (SEM) and optical microscopy (OM)) indicated phase separation phenomena occurence for a CER content of 40% in the SIPN structures. Miscibility studies were conducted by applying the Fox and Gordon–Taylor equations and the results were in good correlation with the data obtained from the characterization methods. Cross–linking densities were determined and their values increase with heat capacity values decrease.

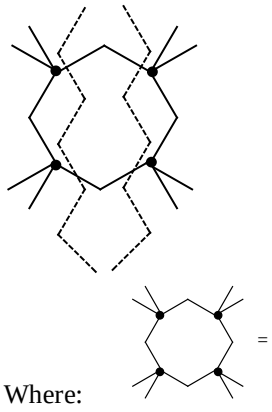

Where:
n = 0.56

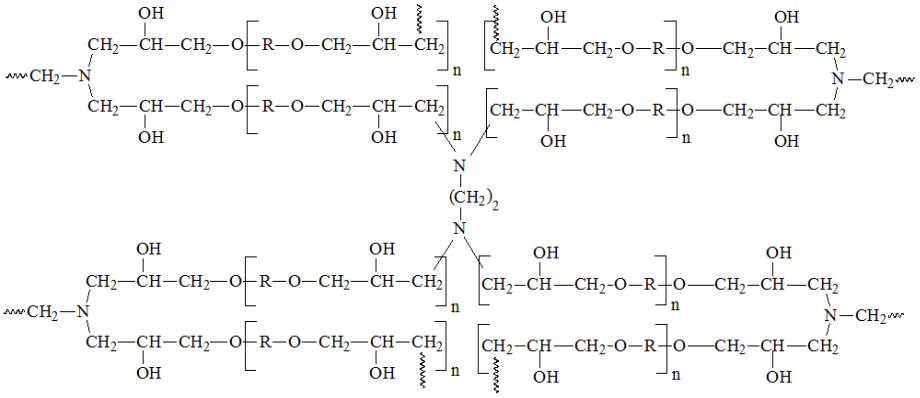

Where :

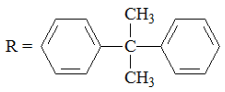

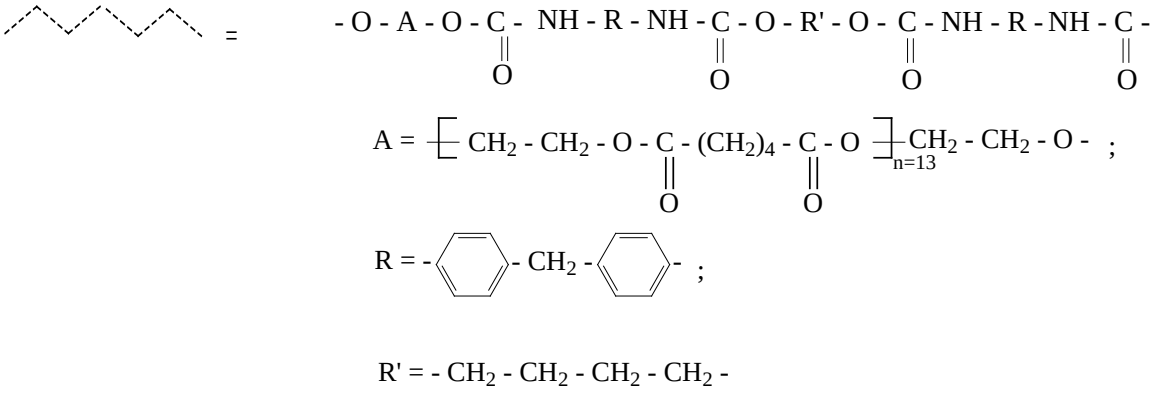

Scheme 3.1. SIPN structure, obtained by inclusion of linear polyurethane in the crosslinked epoxy resin.

Thermal stability studies

Figure 3.7. shows the thermogravimetric (TG) and their corresponding first derivative (DTG) curves of SIPN samples compared with those of PUR and CER polymers recorded at a heating rate of 10°C min^{-1} and in nitrogen atmosphere. The figure shows that the samples thermostability depends on the concentration of crosslinked resin. Samples containing up to a maximum of 10% epoxy resin start decomposing at temperatures between those of pure components. This signifies the existence of some specific interactions between the crude comprising contents.

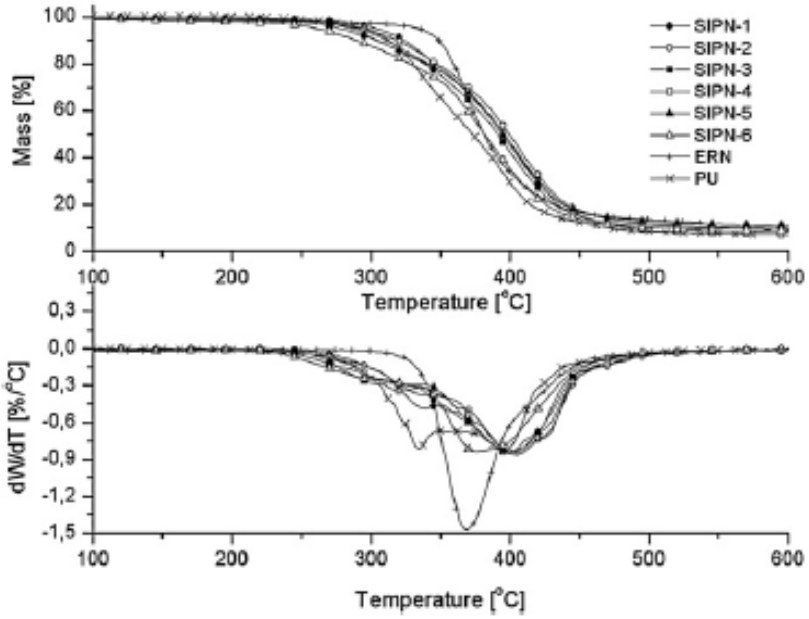

Figure 3.7. TG and DTG curves recorded at 10 °C min^{-1} in nitrogen.

Kinetic analysis

For calculus of kinetic parameters that characterize the thermal decomposition of SIPN samples, such as the preexponential factor (A) and activation energy (E_a), the isoconversional methods of Friedman and Flynn–Wall–Ozawa (OFW) were used.

The thermal decomposition in at least three successive stages is confirmed by the slope of the straight lines variation in Figure 3.10a. The straight lines from Figure 3.10b are not parallel. So, the assumption of a first order reaction for ($f(\alpha) = 1 - \alpha$) function is not the best option in describing the thermal decomposition process. Both isoconversional methods indicate the dependence of the activation energy on the conversion degree. The E_a values ranged between 121 and 211 kJ mol^{-1} for the Friedman method and 107–230 kJ mol^{-1} for the OFW method. The differences between kinetic parameters calculated using Friedman and OFW methods were explained in the literature. The increase of the E_a values with α during heating of SIPN samples may be correlated with a complex thermal degradation mechanism.

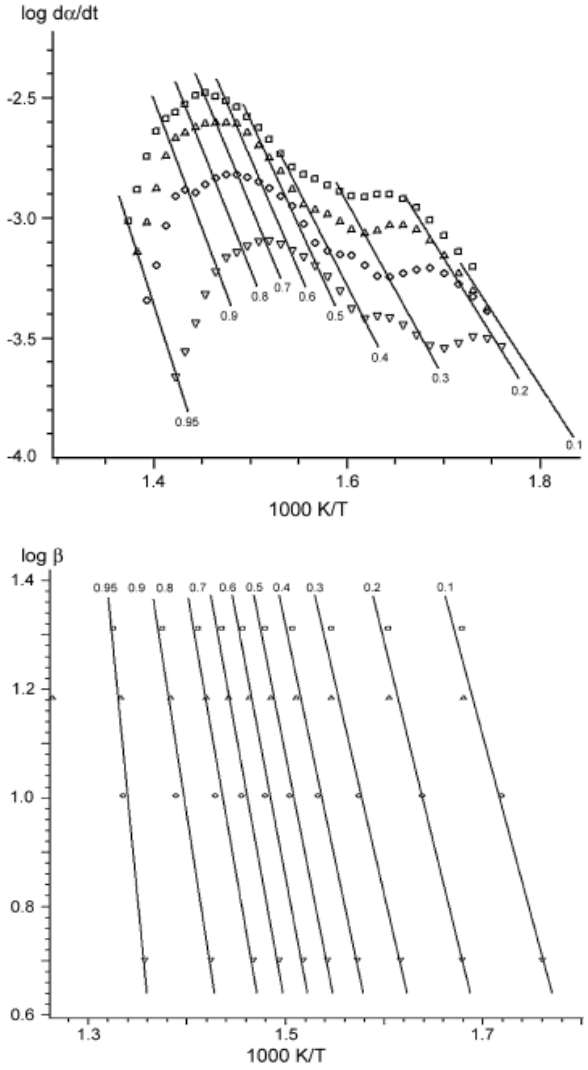

Figure 3.10. Plot of log$d\alpha$/dt as a function of 1000/T according to Friedman method for SIPN4;

(b) Plot of logβ as a function of 1000/T according with OFW method for sample SIPN4.

Since all analyzed samples exhibited a similar thermal behavior to that of SIPN4, a kinetic model in three stages of decomposition was proposed (Eq. (3.11)), where sample (A) is transformed into the solid residue (D) through the intermediate stages (B) and (C) and the corresponding gaseous products

$$A \xrightarrow{1} B \xrightarrow{2} C \xrightarrow{3} D \qquad (3.11)$$

A multivariate non–linear regression software was applied to find the real form of the conversion function. The software optimizes the differential equations parameters and fit them to the experimental thermograms. After testing of all specific kinetic models described in the literature, the statistic parameters have shown that the best fitting of theoretical equations with the experimental data was obtained with n order conversion function, where n is the reaction order (Eq. (3.12))

$$f(\alpha) = (1-\alpha)^n \tag{3.12}$$

The values of 112 kJ mol^{-1}, 112 kJ mol^{-1} and 206 kJ mol^{-1} obtained with the multivariate non–linear regression method correspond to the DTG curve peaks of each individual stage of thermal decomposition. The found values were within the range of the global kinetic parameters determined by the two applied isoconversional methods. Multivariate non–linear regression method fits the experimental data by simultaneously testing of the three kinetic parameters (E_a, A and n) for each stage of thermal decomposition.

The kinetic parameters of SIPN samples are dependent of the CER content in a great extent. The reaction order values indicated changes in the thermal degradation mechanism with increasing of CER content in SIPN samples. Values of $n > 2$, which characterize the first stage of thermal decomposition in SIPN1 and SIPN2, indicate the mass loss related to the intermolecular transfer and scission of the network structure. Increasing of CER concentration above 10% changed the n value to ≈1, indicating the mass loss by random scission probably located in the main chain of the polyurethane.

The evolved gas analysis, measured through a TGA–FTIR–MS coupling, indicated that the main found gases in the mixture were ammonia, carbon oxides, water vapours, alcohols and oxigen traces.

Photochemical behavior of semi–interpenetrating polymer networks based on polyurethane and epoxy resin

In this section, there is presented a brief overview of the major modifications of some SIPN properties during UV irradiation, in correlation with the samples structure, monitored via changes in FTIR spectra.

The gloss retention (G_r) on the surfaces of the samples was calculated by comparing the intensity of luminous reflection on the sample surface with the value obtained for the standard (polished black glass) with Eq. (3.14), where G_i and G_f represent the initial and the final gloss values.

$$G_r = \frac{G_f}{G_i} \cdot 100 \tag{3.14}$$

The lowest value of gloss retention was found for the PUR sample (48.7). The SIPNs were characterized by values of gloss retention ranging between 76.9 (SIPN2) and 96.1 (SIPN4). The decrease of G_r on SIPNs surface during irradiation may be explained by changes in their roughness, because there is a direct relationship between gloss and roughness. It is well known that the rough surfaces are less glossy. An explanation of the higher decrease of gloss of the polyurethane sample compared with SIPN samples is the high transparency of the polyurethane film. Therefore, the UV light deeper penetrates the PUR structure, generating an advanced deterioration of the film.

Photometry is the optical sciences branch which is focused on the measurement of optic radiations exactly as percieved by the human eye. In 1931, the CIE ("Commission Internationale de l'Eclairage") introduced a standard regarding the medium response given by the human eye in normal illuminating conditions, with a 2^o observation field. Thus the basis of RGB system had been established, representing an attempt to recognize and describe the percieved colors by using three sensibility curves which characterize the colors red, green and blue. It was thereby considered that, by mixing the three fundamental colors, any other color could be completely described. Most of the color models possess three components: the lightness factor, tone and saturation. The three constituents may be represented by including them in a sphere (Scheme 3.2).

The necesity of representing colors through numerical reproducible values and void of subjective influences regarding device construction and observer qualities has determined the CIE to request the introduction of the CIE$L^*a^*b^*$ system in 1976. In the CIE$L^*a^*b^*$ system the colors of the visible spectra are expressed within a threedimensional space and on three perpendicular directions. Each color may be reproduced by combining the L^*, a^* and b^* parameters. In this system, on the vertical axis there is represented the lightness factor (L^*). L^* is an adimensional size which varies between the limits 100 and 0, values characterizing the colors white (100) and black (0). The chromatic coefficients a^* and b^* are represented on the two horizontal and perpendicular directions. Chromatic coefficient a^* describes the positioning of the color on a scale between the value – a, representing pure green, and the value + a, representing pure red. Chromatic coefficient b* also ranges

between the same limits, except that value – b represents pur blue, while the value + b corresponds to pure yellow.

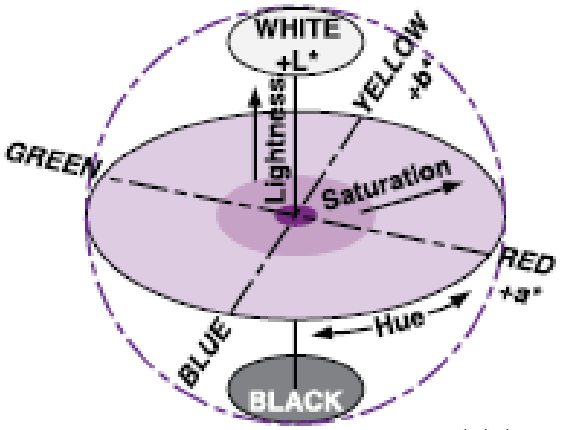

Scheme 3.2. Color space in the CIEL*a*b* sytem.

Color modifications (ΔE) (Eq. (3.15)) were evaluated by monitoring the lightness factor (L^*) values and chromatic coordinates of redness and yellowness (a^* and b^*) variation before (L_1^*, a_1^*, b_1^*) and after (L_2^*, a_2^*, b_2^*) UV irradiation.

$$\Delta E = \sqrt{(L_2^* - L_1^*)^2 + (a_2^* - a_1^*)^2 + (b_2^* - b_1^*)^2} \qquad (3.15)$$

The lightness factor decreased for all the studied samples during irradiation, which is an indication of the darkening of all samples after UV irradiation (Figure 3.19). The irradiation caused the increase of chromatic coefficients values (a^* and $b^{*)}$ for all the studied samples (Table 3.7). The chromatic coordinates variation shows the tendency of reddening and yellowing of the irradiated samples. Accumulation of chromophore compounds with extended conjugation structure such as the ones resulting from photodegradation of PUR or/and of CER may explain the color changes on the films surface. After 200 h irradiation time the samples changed the color from grey to brown due to darkening and accumulation of red and yellow chromophores on the surfaces.

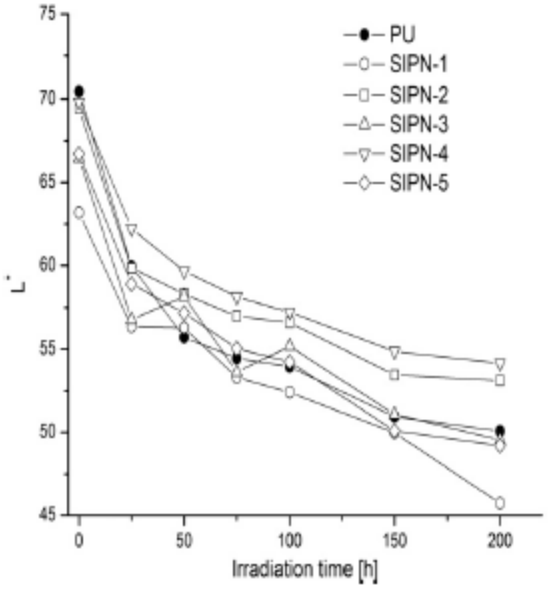

Figure 3.19. Variation of the lightness factor with irradiation time.

The contact angles of water on the surface of studied samples changed during irradiation. In the first 100 h of irradiation the contact angle of water on the surface of irradiated samples significantly decreased.

Formation of some oxidation products and ortho–amino ester structures as a result of photo–Fries rearrangement in urethane bond (Scheme 3.3) could increase the affinity of water for the SIPNs irradiated surface. The decrease of surfaces polarity due to the accumulation of some saturated and unsaturated hydrocarbon structures resulted from the photodecomposition of aliphatic ester in PUR by Norrish type reactions (Scheme 3.3) may explain the increase of the contact angle above the initial values after 200 h of irradiation.

Table 3.7. The variation of chromatic coefficients with irradiation time.

Sample	a^*							b^*						
	0	25	50	75	100	150	200	0	25	50	75	100	150	200
PUR	-0.57	1.563	2.135	3.750	4.243	4.314	4.421	11.680	30.864	31.001	31.371	31.790	34.532	35.012
SIPN1	0.291	0.868	0.902	1.003	1.063	3.241	7.194	13.503	22.103	23.798	24.802	25.558	27.101	29.798
SIPN2	-2.49	1.257	1.474	2.003	2.273	5.668	6.001	16.795	22.343	23.111	26.115	27.972	28.003	28.595
SIPN3	-2.20	0.013	0.423	0.585	0.814	0.951	0.963	15.928	17.324	19.235	22.043	24.143	25.005	25.870
SIPN4	-1.49	0.023	0.520	1.243	1.827	3.353	5.380	11.959	19.222	23.384	25.252	26.095	27.312	28.224
SIPN5	2.278	2.345	2.446	2.502	2.588	4.582	6.300	16.925	17.555	22.128	25.399	29.282	28.887	28.420

The FTIR spectra of SIPNs show both characteristic signals for PUR and for CER network. As an exemplification, Figure 3.20 presents the FTIR spectrum of SIPN3 compared with the spectra of PUR sample and of CER network. The large signal from 3200 to 3600 cm^{-1} with the peak at 3324 cm^{-1} from Figure 3.20c characterizes the stretching vibration of O–H group in the CER network and the stretching vibration of N–H group in PUR. Also, the signals from 2958, 2924 and 2870 cm^{-1} can be assigned to the valence vibrations of the C–H bonds from CH_2, CH_3 and CH structures in CER network and PUR. The signals from 1728 to 1703 cm^{-1} characterize the PUR. The signal from 1728 cm^{-1} is specific to the C=O stretching vibration of ester structure while the peak from 1703 cm^{-1} corresponds to C=O stretching vibration from urethane bond (amide I band). The signals from 1598 cm^{-1} and 827 cm^{-1} characterize the aromatic structures from PUR and from the epoxy CER network. The first signal was allocated to the skeletal vibrations of C=C double bonds in aromatic ring and the second signal to the C–H out of plane bending vibrations in 1,4–disubstituted aromatic ring. The absorbance from 1530 cm^{-1} was attributed to the coupling of N–H bending vibration with the C–N stretching vibration in the C–NH group in PUR (amide II band) and the shoulder from 1511 cm^{-1} could be associated with the aromatic ring from CER network. The signals from 1461 and 1413 cm^{-1} are specific bands (υCH2) in PUR structure and in CER network and the weaker band from 1309 cm^{-1} corresponds to amide III band (a combination between the C–N stretching vibration and N–H bending vibration) in PUR. The range 1300–1000 cm^{-1} is assigned to several chemical structures. This range of wavenumbers can characterize both the stretching vibration of C–O bond of ester from PUR and the aryl alkyl ether units from CER network.

Several major changes in the FTIR spectra of samples were observed after UV exposure. Figure 3.21 presents, as an exemplification, the FTIR spectra of SIPN3 sample recorded before (A), after 200 h of irradiation (B) and the difference between the two spectra (C).

The difference spectrum (Figure 3.21, spectrum C) exhibits positive and negative signals. The positive intensities show the structures that were lost during irradiation. Decreases in intensities of these bands indicate that the chain scission and mass loss in the films have taken place during the UV exposure. In the case of SIPN samples the decrease in the following signal intensities during irradiation has been observed: 3324, 2954, 1727, 1535, 1514 and 1277 cm^{-1}. The decreasing in intensity of the signals from 3324 to 1535 cm^{-1} indicates the structural degradation of PUR through photo–Fries rearrangement when ortho–aromatic aminoester structures resulted (Scheme 3.3).

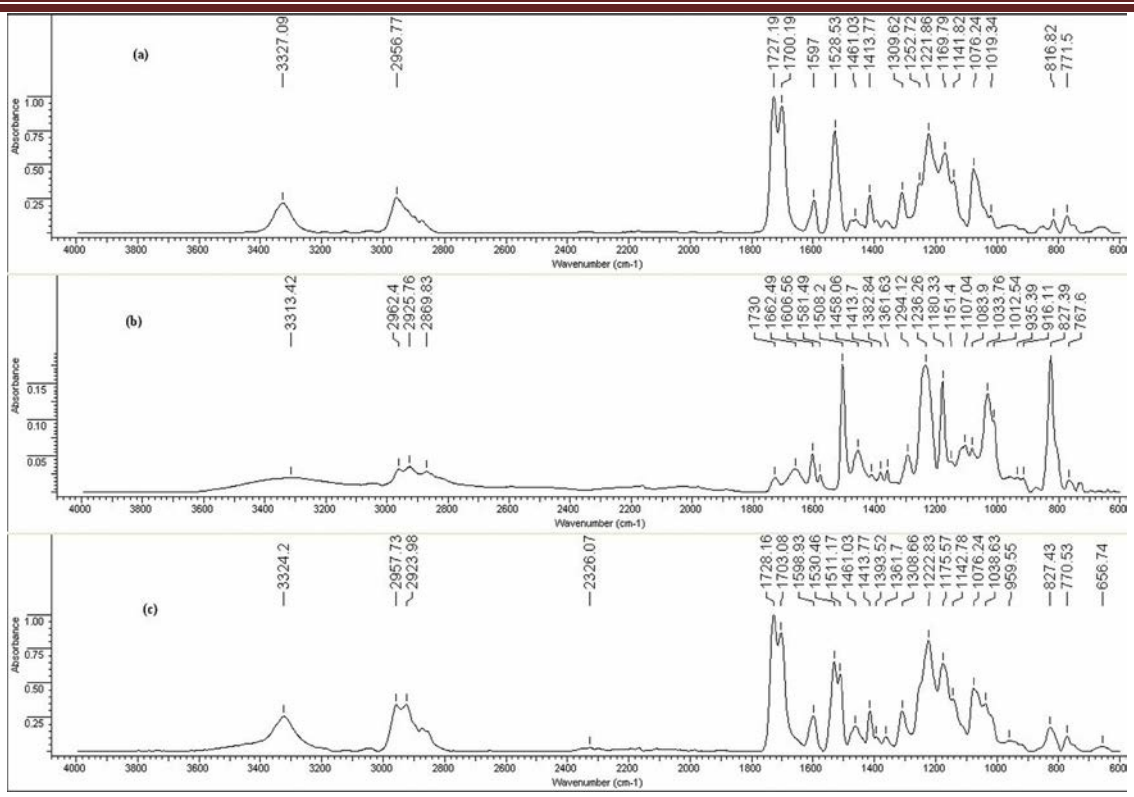

Figure 3.20. The FTIR spectra of: PUR sample (a); CER network (b) and of SIPN3 (c).

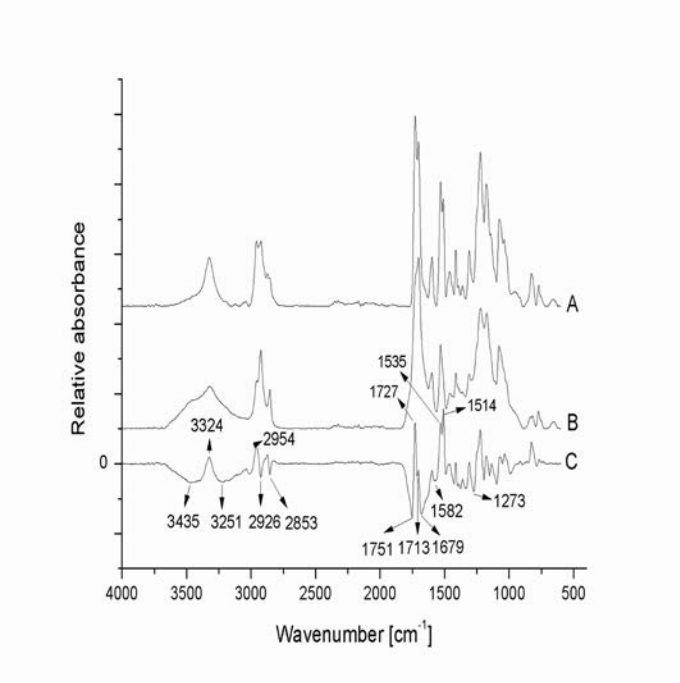

Figure 3.21. The FTIR spectra of SIPN3 recorded before irradiation (spectrum A), after 200 h irradiation time (spectrum B) and the difference between A and B (spectrum C).

Figure 3.22 presents the variation of the surface of signal between 1492 and 1570 cm with the peak at 1535 cm^{-1}, during irradiation. Figure 3.22 shows that the largest changes occur in the first 25 h irradiation time. After 200 h of irradiation the most important loss of urethane bonds took place in PUR structure because of the photo–Fries rearrangement. The explanation for this behavior can be related with the higher transparency of PUR film versus SIPN structures that are more opaque. The UV radiations are partially absorbed by the epoxy network or are hindered to penetrate in depth of the film sample having the effect of urethane polymer protection. The decreases of signals from 2954 to 1727 cm^{-1} show the photodegradation of aliphatic ester structures from polyurethane by Norrish type reactions (Scheme 3.3).

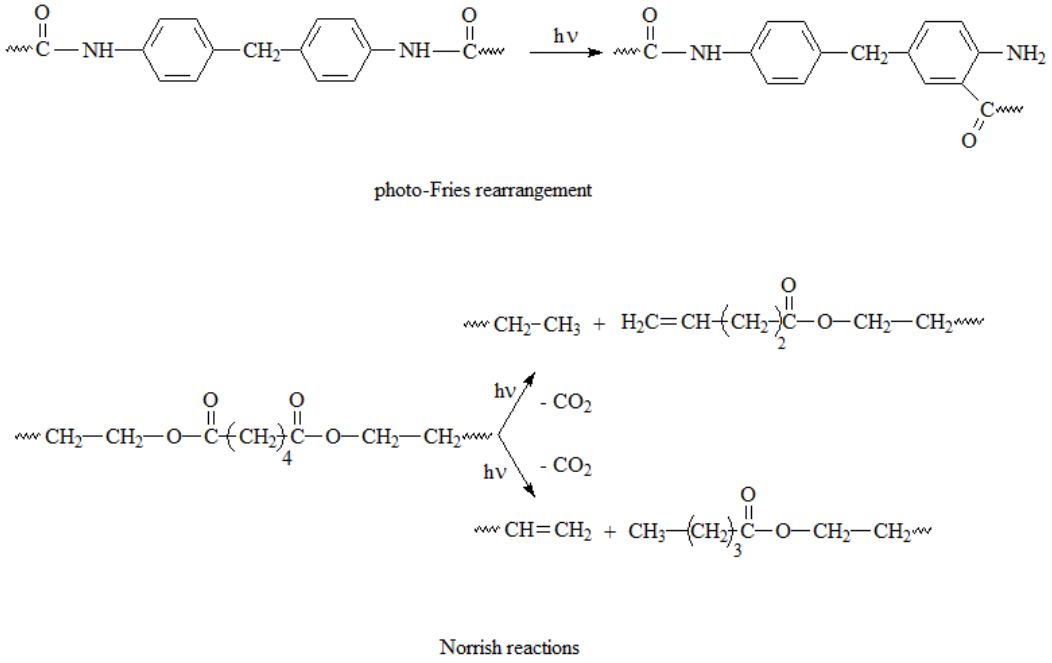

Scheme 3.3. Photodegradation mechanism of PUR.

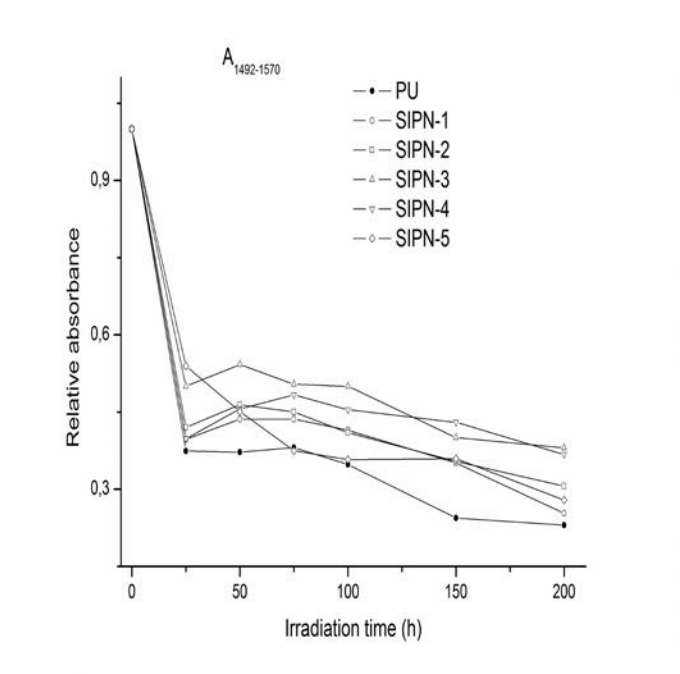

Figure 3.22. Variation of absorbance from 1535 cm^{-1} with irradiation time..

Modification of the surface signal between 1716 and 1750 cm^{-1} with the peak at 1727 cm^{-1} during irradiation is presented in Figure 3.22. The significant decrease of absorbance specific to ester structure with the peak at 1727 cm^{-1} can be also observed in the first 25 h of irradiation. The largest losses of ester bonds were found in the PUR and SIPN5 samples. It can be observed from Figure 3.23 that the increasing in CER content up to 20% protects the soft segments in PUR from photodegradation. An explanation is that the samples become more opaque than PUR with CER content increase. An increase of over 20% CER content determines phase separation in islands rich in PUR and CER content. This aspect could explain a tendency in the decrease in carbonyl moieties concentration in soft segments of PUR from sample SIPN5 during irradiation.

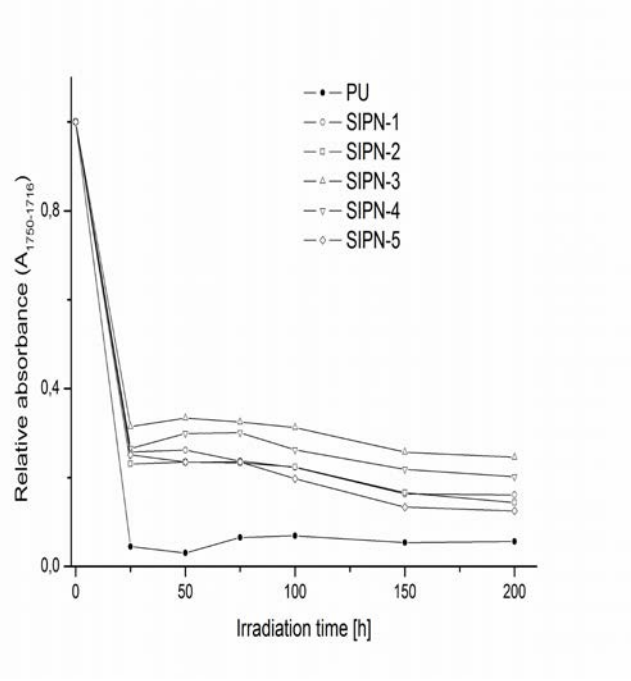

Figure 3.23. Specific absorbance variation of ester structure from 1727 cm^{-1} during irradiation.

Photodegradation of ester structures by Norrish type reactions occurs by removing of carbon dioxide which means mass variations of studied samples. The studied samples have lost between 1.2 and 1.7% of their initial weight after 200 h irradiation time. This behavior can be explained by the release of some volatile compounds during photodegradation as is the carbon oxides. CER network photodegradation is supported by the presence of signals from 1250 to 1511 cm^{-1} in the difference spectra. In addition to the decreasing intensity of certain bands, some negative signals at 3435, 3251, 2926, 2853, 1751, 1713, 1679, 1582 and 1723 cm^{-1} have appeared in spectrum C from Figure 3.21. The signals indicate the formation of new chemical species during the photodegradation of SPINs. Thus, the two peaks from 3435 to 3251 cm^{-1} characterize the stretching vibration of N–H bonds in primary amine appeared as a result of photo–Fries rearrangement in PUR. The large signal between 1620 and 1800 cm^{-1} with the two peaks located at 1751 and 1713 cm^{-1}, visible in difference of spectra from Figure 3.21, indicate formation of chemical compounds with high polarity (peroxides, aldehydes, ketones or acids) as a result of photo–oxidation process of SIPNs.

Presence of primary amine groups and of the oxidation products in irradiated samples structures increases the water retention in SIPNs. This behavior is normal. Increasing the concentration of CER network enhances the OH group number in SIPN structure which is able to interact with water molecules. A higher number of OH groups mean more retained water. Formation of chemical structures with high polarity as a result of photochemical and photo–oxidation processes further increases the amount of water retained.

INFLUENCE OF POLY(VINYL ALCOHOL) ON CELLULOSE PHOTOCHEMICAL STABILITY IN CRYOGELS DURING UV IRRADIATION

The composition of the cryogels used in the study is given in Table 4.1.

Table 4.1. Cryogels composition.

Sample	Composition (%)	
	PVA	Cellulose
PVA	100	0
90/10	90	10
70/30	70	30
50/50	50	50
Cellulose	0	100

Significant color changes were found during irradiation. A fading trend of samples with increase of irradiation dose was observed. Figure 4.1 shows that the lightness factor (L^*) increases with irradiation dose. The most important changes in L^* values were recorded for cellulose ($\Delta L^* = 14.99$) and PVA ($\Delta L^* = 10.54$) at the highest irradiation dose value (1266 J cm^{-2}). A slow variation of L^* was recorded up to 584 J cm^{-2} irradiation dose, or 120 h irradiation time respectively, for both polymers which indicated the presence of an induction time or of a critical dose of irradiation. As soon as the induction period or the critical irradiation dose was exceeded, a sharp increase of L^* occurred. The variations of L^* values with irradiation dose for PVA/cellulose cryogels were much lower than for the starting polymers. ΔL^* values recorded at maximum irradiation dose values for each sample decreased with the increasing of cellulose content in the mixture.

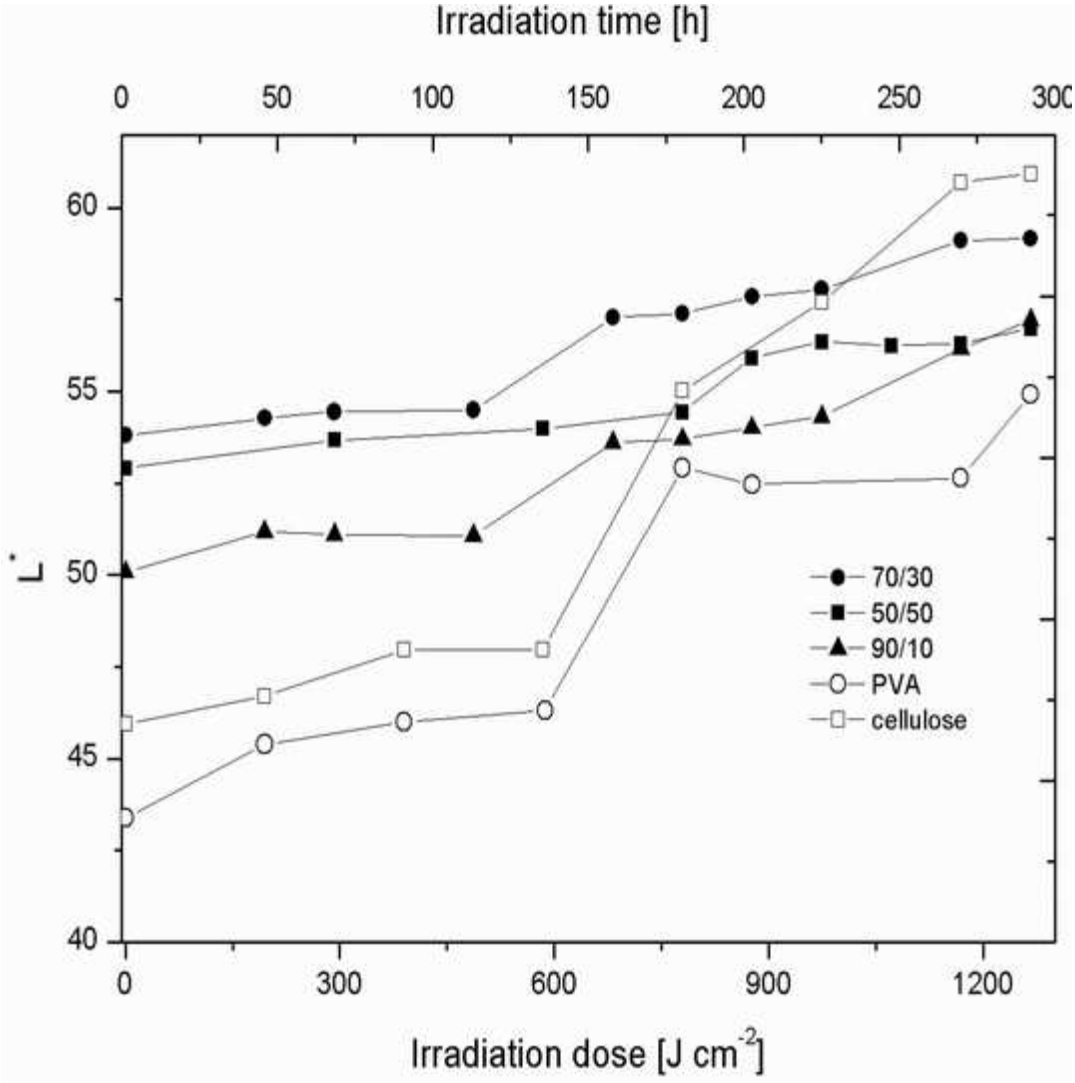

Figure 4.1. Variation of lightness factor with irradiation dose.

Figures 4.2 and 4.3 show the variation of the chromatic coefficients a^* and b^* during irradiation. It can be observed from Figure 4.2 that pure cellulose exhibits a slow increase in a^* values in the range 195–390 J cm^{-2} irradiation dose (40–80 h irradiation time) due to small amounts of red chromophores accumulated on the surface. After the accumulation of these chromophores, cellulose exhibits a stable plateau for a^* values after an irradiation dose value of 390 J cm^{-2} (80 h irradiation time). The b^* values (Figure 4.3) variation shows the tendency of yellowing of pure cellulose during the whole irradiation process due to the continuous accumulation of yellow chromophore compounds. Figure 4.2 shows that, unlike cellulose, pure PVA exhibits a different photochemical behavior. This aspect can also be noticed for all the cryogels which exhibit the same trend. The photochemical behavior trend can be divided in two stages. The former stage, up to 80 h (390 J cm^{-2} irradiation dose), consists in a fast accumulation of instable red chromophores which start decomposing in the latter stage. Figure 4.3 shows a continuous increase of b^* with irradiation dose of PVA, due to surface yellowing.

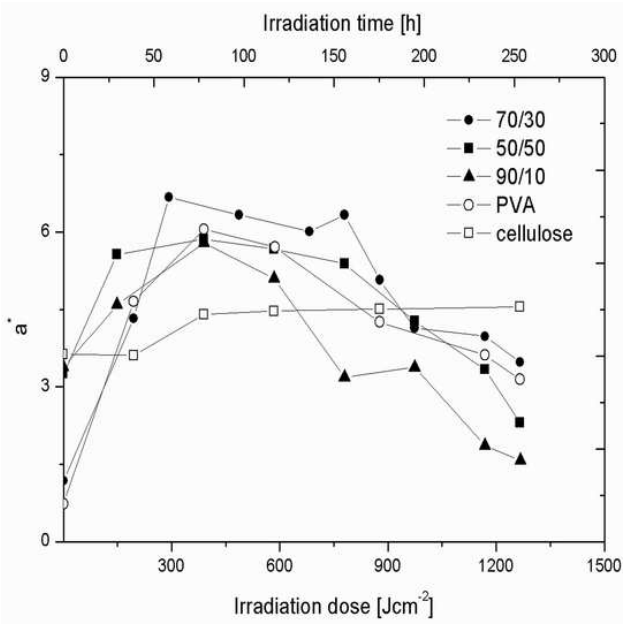

Figure 4.2. Variation of chromatic coefficient a^* with irradiation time.

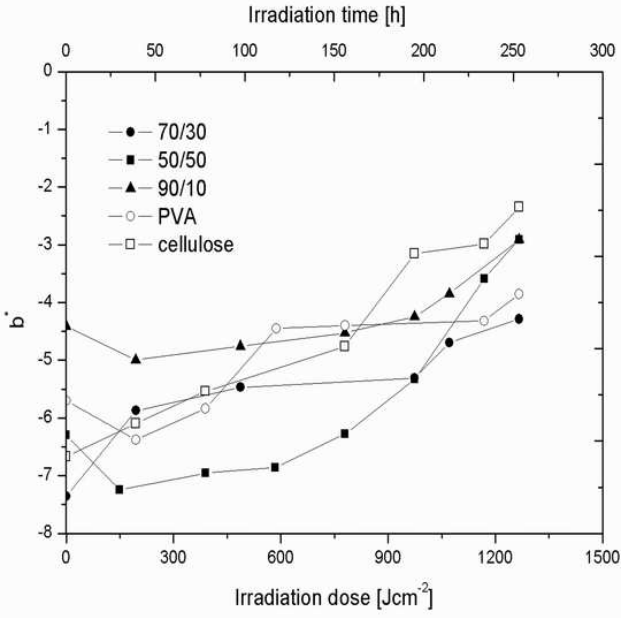

Figure 4.3. Variation of chromatic coefficient b^* with irradiation time.

Structural modifications of cryogels during UV irradiation

FTIR analysis

Figure 4.5 depicts the FTIR spectra before irradiation, after 260 h irradiation time (1266 J cm^{-2} irradiation dose) and the difference spectrum for the pure PVA (Figure 4.5a), cellulose (Figure 4.5c) and the cryogel containing 30% cellulose (Figure 4.5e). As an exemplification, structure containing 30% cellulose was taken into account, due to the other cryogels similar photochemical behavior. The FTIR spectra show important structural modifications during irradiation. The difference spectra display positive and negative signals. The positive signals indicate the structures lost during irradiation, whilst negative signals indicate the formation of new structures. Signals decrease indicates that photodegradation occurred through mass loss and chain scission .

It can be observed that the FTIR spectrum of sample containing 30% cellulose (Figure 4.5e) contains absorption bands of both comprising polymers. Furthermore, both constituents of the cryogels exhibit absorption bands specific to carbonyl groups, which are generally known as significant initiating sites for photodegradation phenomena.

The peaks at 3447 cm^{-1} and 1634 cm^{-1} in the difference FTIR spectrum of PVA (Figure 4.5a) indicates loss of OH and C=O structural entities during irradiation. The new peak at 3649 cm^{-1} corresponds to hydroperoxide formation, confirmed by the iodometric method with a value of $25 \cdot 10^{-4}$ mol (–OOH)/g polymer. The peak at 3159 cm^{-1} may be an indication of mainly acidic OH entities formation as a result of PVA depolymerization. The appearance of new signals at 1580 cm^{-1} and 1402 cm^{-1} were attributed to C–H bending vibration and C=C stretching vibration from newly formed unsaturated structures.

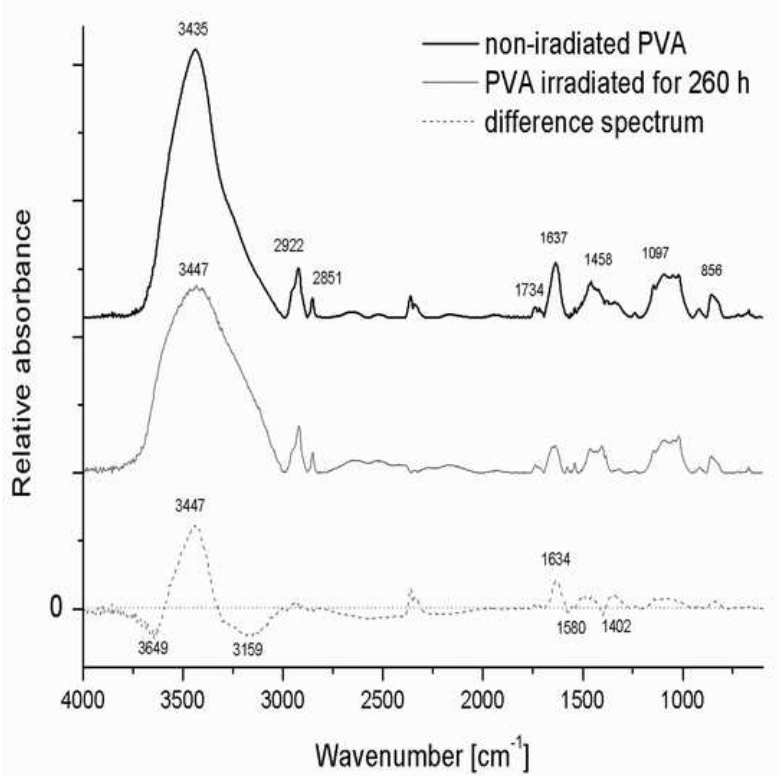

Figure 4.5a. FTIR spectra of PVA.

Figure 4.5b displays the carbonyl region in the FTIR spectrum of non–irradiated PVA and PVA after 260 h irradiation time. A general decreasing trend may be observed in the carbonyl region of irradiated PVA, indicating mass loss by depolymerization processes during photoirradiation. The absorbtion band with a peak at 1717 1 cm^{-1} is characteristic to ketones. This band decreased in intensity due to the low photostability of the formed ketones which undergo photochemical decomposition by Norrish I reactions with CO evolvement. Gaume and co–authors analyzed the oxidation photoproducts during photoirradiation of PVA after 6000 h irradiation time by various characterization methods and found a mixture comprised of the following compounds: tartaric acid, succinic acid, malonic acid, lactic acid, propionic acid, acetic acid, formic acid and oxalic acid. This aspect explaines the decrease and broadening in intensity of the irradiated PVA spectrum in the range 3000–3800 cm^{-1} from Figure 4.5a. The presence of acetic acid, amongst other photooxidation products, was explained by other authors, by a Norrish II mechanism of poly(vinyl acetate) irradiated at λ>300 nm, with formation of C=C unsaturated entities in the main chain . This aspect may also be available for the remaining acetate groups during PVA backbone photocleavage, explained by the lowering in intensity of the carbonyl region. Also the impurities and/or oxidation products formed during preparation and processing may represent important initiating sites for photooxidation. The new peak at 1578 cm^{-1} , which is significantly intense and broader for the irradiated PVA, corresponds to the C–H stretching vibration adjacent to C=C bonds newly generated unsaturated structures resulted during photoiradiation. This peak confirms the correct attribution of the peak at 1580 cm^{-1} in the difference spectrum in Figure 4.5a, to C=C unsaturated structures. The peak at 1734 cm^{-1} corresponds to the acetate moietes and/or oxidation during preparation and processing of the polymer in the

non–irradiated PVA spectrum. Its lowering in intensity in the spectrum of the PVA irradiated for 260 h is attributed to the cleavage of acetate moieties which generate acetic acid through Norrish II reactions. The peak at 1701 cm^{-1} had considerably lowered in intensity in the spectrum of the PVA irradiated for 260 h. This aspect was explained by the formation of unsaturated aldehyde entities during photoirradiation.

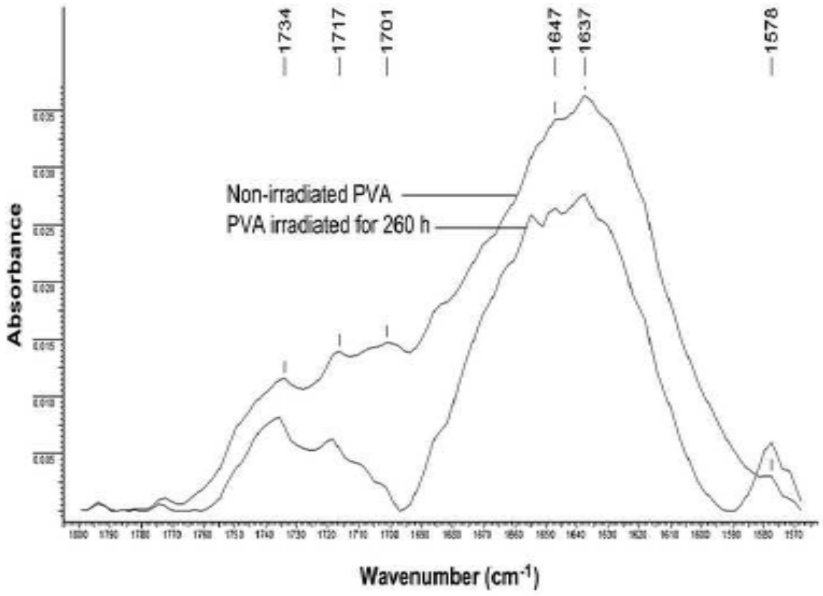

Figure 4.5b. Carbonyl region in the FTIR spectrum of non–irradiated PVA and PVA after 260 h irradiation time.

The difference FTIR spectrum of cellulose (Figure 4.5c) indicates the occurring of intense photooxidation processes during irradiation. The broad signal containing multiple peaks in the range 3150–3623 cm^{-1} corresponds to the formation of new hydroperoxidic structures. The new broad peak in the range 1522–1837 cm^{-1} confirms the occurrence of photoxidation processes via the formation of new carbonyl structures.

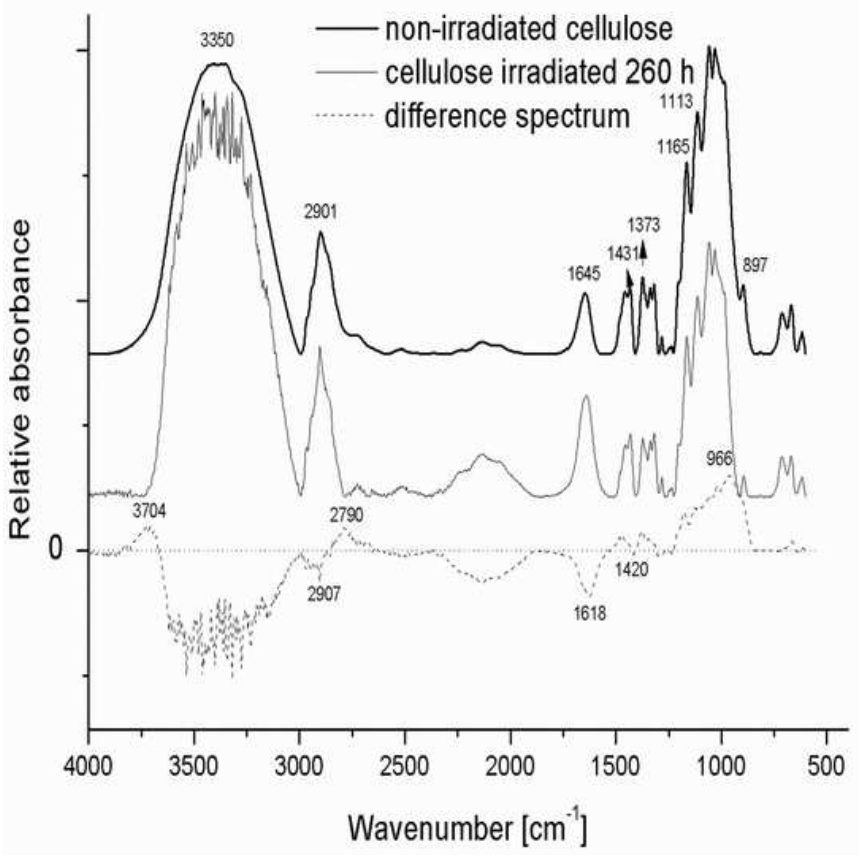

Figure 4.5c. FTIR spectra of cellulose.

By applying the second derivative a deconvolution was possible, leading to the identification of four previously overlapped signals with peak values at 1630 cm^{-1}, 1665 cm^{-1}, 1685 cm^{-1} and 1727 cm^{-1}, as one may observe in Figure 4.5d. The signal at 1630 cm^{-1} is attributed to the formation of some C=C bonds possibly conjugated with other double bonds or carbonyl and/or carboxyl groups resulted during cellulose photodegradation. The peak at 1665 cm^{-1} is attributed to C_2–C_3 α–diketones formation which may undergo keto–enol tautomerism. These diketones are responsible for cellulose yellowing and their formation occurs regardless of hydrolysis phenomena in the main cellulose backbone. From Figure 4.5d there may also be observed a weak signal at 1650 cm^{-1} attributed to C=C stretching vibration which is often masked by the water absorption band at the same frequency. The signal at 1685 cm^{-1} corresponds to photooxidation of C_6 from cellulose structure which, together with internal dehydration, generates αβ–unsaturated aldehydes, again with the peak at 1650 cm^{-1}. Further photocleavage of the cellulose C_2–C_3 bonds leads to conjugated unsaturated structures which are further lost during irradiation, this being a specific photoreaction of cellulose under sunlight exposure. In this sense, the signal peak at 1727 cm^{-1} may correspond to aliphatic aldehyde structures. The decrease in the intensity of signals in the region 1113–897 cm^{-1} with a peak at 966 cm^{-1} in the difference spectrum may be attributed to cellulose depolymerization by glycosidic bonds cleavage. The decrease in absorption bands with peak values at 2790 cm^{-1} and 3704 cm^{-1} may correspond to some dehydration along with the formation of C=C bonds.

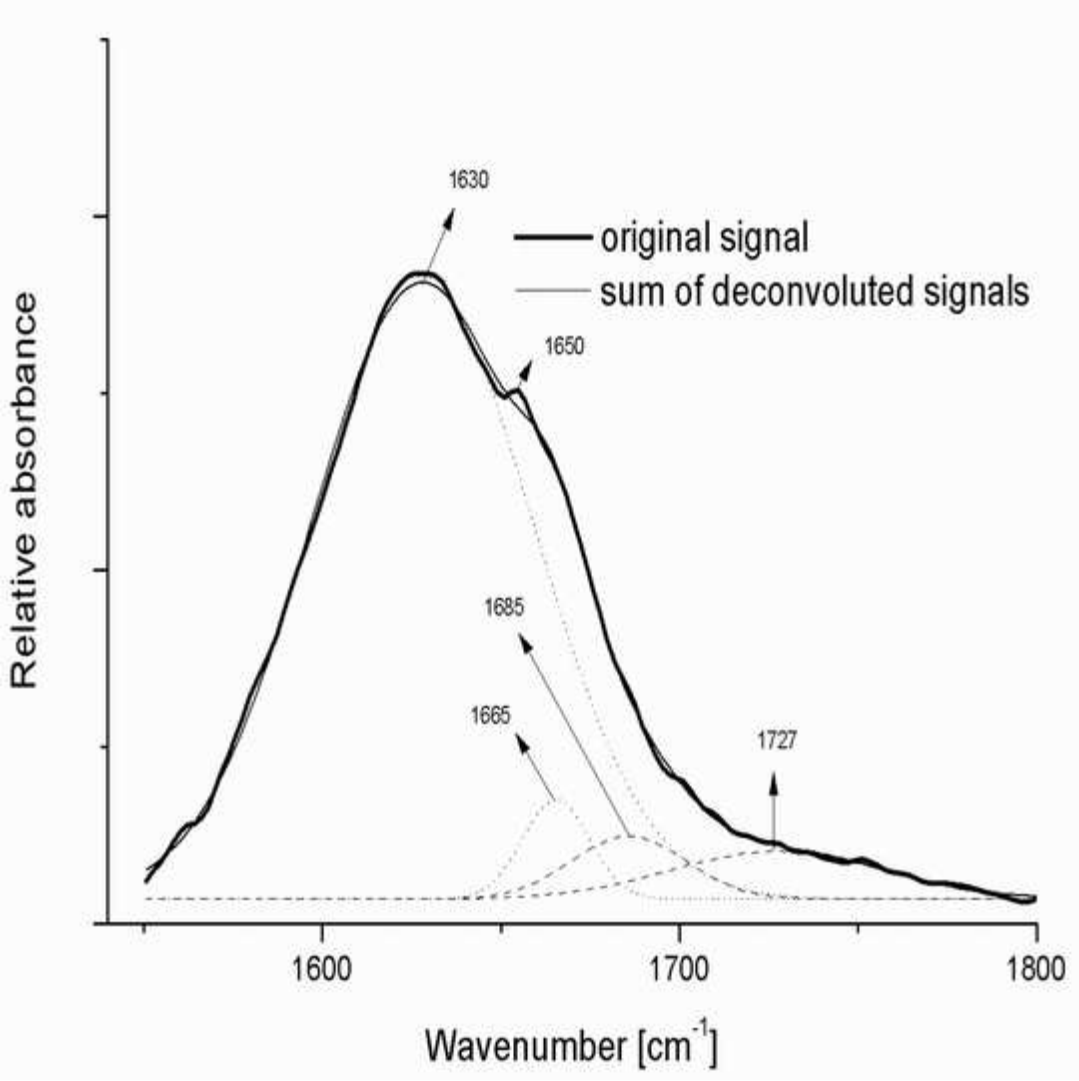

Figure4.5d. Deconvoluted peaks in the range 1500–1800 cm^{-1} for photodegraded cellulose.

It may be observed from the difference spectrum in Figure 4.5e that during photodegradation of sample 70/30, no significant new entities were formed, rather especially depolymerization processes occurred, leading to a decrease in intensity for all signals.

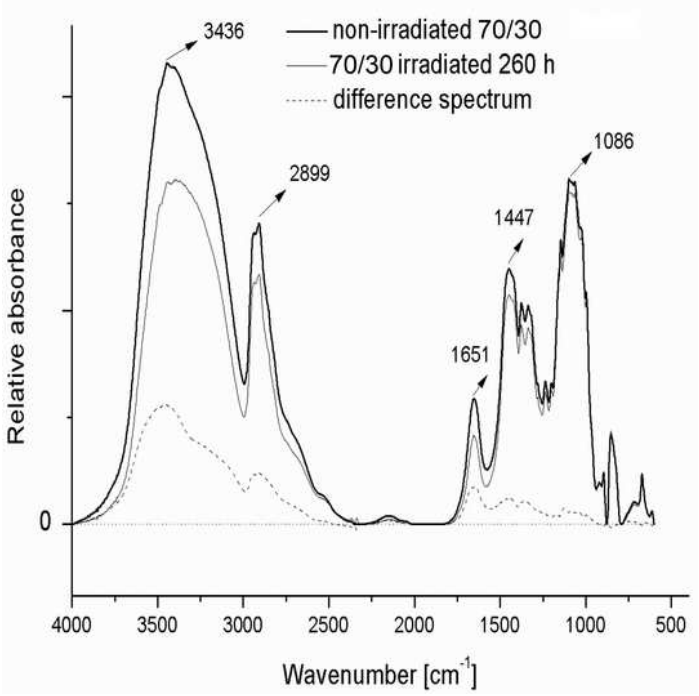

Figure 4.5e. FTIR spectra of cryogel 70/30.

XPS analysis

XPS spectra of pure components and of 70/30 cryogel showed, as expected, carbon (C_{1s} at 285 eV) and oxygen (O_{1s} at 532 eV) atoms as the two major constituents. Figure 4.7 displays the C_{1s} deconvoluted peaks of sample 70/30 before and after 260 h irradiation time. The C_{1s} deconvolution results of both comprising polymers and that of cryogel 70/30 before and after 260 h irradiation time are summarized in Table 4.3.

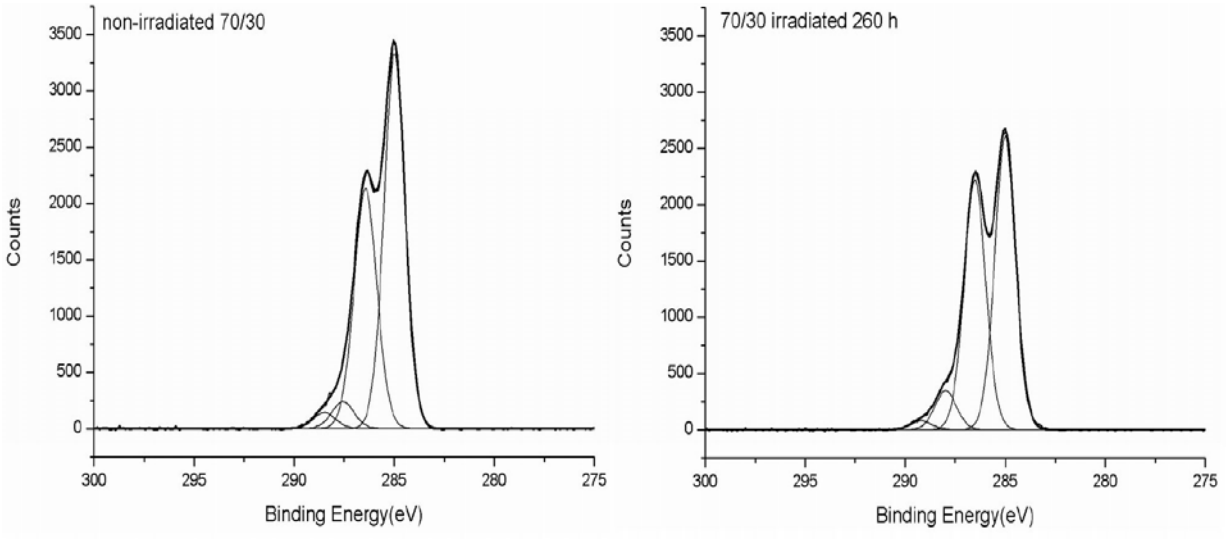

Figure 4.7. C_{1s} fitted curves of cryogel 70/30 before and after 260 h of photooxidation.

One may observe from Table 4.3 that photooxidation led to a decrease in C–C and C–H entities from the 70/30 cryogel. This aspect is due to the oxidation of the alkyl chains. Also, an increase in moieties containing C–O bonds may be noticed. The formation of new hydroperoxidic structures during photooxidation of 70/30 cryogel may explain this behavior. The oxdation of alkyl chains from the cryogels occurs simultaneously with continuous hydroperoxide formation. The increase in C=O bonds content may be explained by new carbonylic groups formation during photooxidation. A significant decrease in O–C=O content, from residual acetate groups in PVA, after irradiation is due to the Norrish II reaction, leading to acetic acid formation. Oxygen fixation and

formation of oxidized products lead to a slight increase of the O/C ratio in the cryogels after irradiation from 0.378 to 0.389. This aspect is in good agreement with Figure 4.7, which shows that no new peaks were formed during irradiation, and with Figure 4.5e in which the FTIR difference spectrum indicated no significant formation of photooxidative products. All the above mentioned aspects confirm that, up to a concentration of 70%, PVA retards cellulose photochemical decomposition, thus behaving as an oxygen barrier

Table 4.3. Summary of C_{1s} peak deconvolutions (%).

Compound	Binding energy (eV)	Assignment	0 h	260 h
Celullose	285	C–C și C–H	14.24	16.02
	286.6	C–O	66.76	63.62
	288	O–C–O	19	17.57
	298.1	C=O	—	2.79
PVA	285	C–C și C–H	74.71	68.39
	286.4	C–O	20.10	23.23
	287.7	C=O	3.05	4.69
	289.2	O–C=O	2.14	3.69
70/30	285	C–C și C–H	54.89	48.84
	286.4	C–O	38.12	42.80
	287.6	C=O	4.31	6.78
	288.5	O–C=O	2.59	1.58

The main photo–oxidation products traces of the cryogel containing 30% cellulose, identified throguh TG–MS coupling, were: acetic acid, acetone, 2–propenal, propanoic acid, butanoic acid and ethyl methyl ketone.

Photodecomposition mechanisms of PVA and cellulose in cryogels

Based on the data interpretation from all characterization methods mentioned above, Schemes 4.1 and 4.2 depict the proposed photodecomposition mechanisms for celullose and PVA in cryogels.

The impurities and/or oxidation products formed during preparation and processing represent important initiating sites for PVA photooxidation (I), leading to intermediate formation of hydroperoxides (II) which further causing photodecomposition process (Scheme 4.1). New compounds containing double bonds and carbonyl entities, such as ketones (III), are formed during UV irradiation of PVA. The intermediate ketonic compounds undergo photodecomposition process *via* Norrish I type reactions, generating CO evolvement. Also, during PVA photodecomposition, there is formed a series of acid entities such as acetic acid. Acetic acid results from the residual acetate moieties, remained unhydrolyzed in the polymer, through Norrish II mechanism with formation of unsaturated structures in the backbone. New compounds with aldehydic structure arise during UV irradiation, due to internal dehydration.

Cellulose photodecomposition process occurred by photo–oxidation and macromolecular chain scission with indermediate hydroperoxide formation (Scheme 4.2). Formation of some C=C bonds possibly conjugated with other double bonds or carbonyl and/or carboxyl groups results during cellulose photodegradation. There also occurs α-diketones formation at cellulosic C_2–C_3 atoms which may undergo keto–enol tautomerism. These diketones are responsible for cellulose yellowing and their formation occurs regardless of hydrolysis phenomena in the main cellulose backbone. Photooxidation of C_6 from cellulose structure, together with internal dehydration, generates αβ–unsaturated aldehydes. Further photocleavage of the cellulose C_2–C_3 bonds leads to conjugated unsaturated structures which are further lost during irradiation.

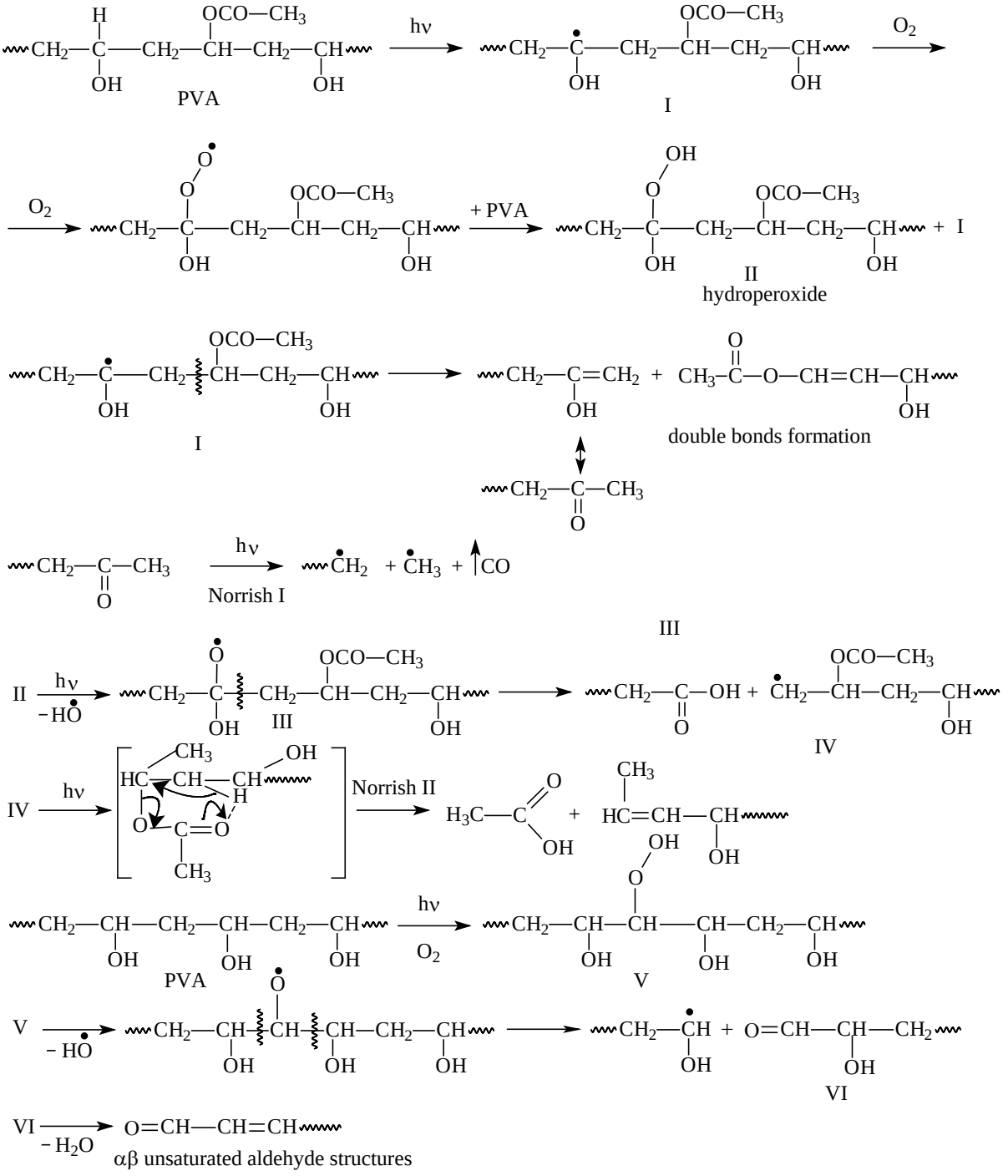

Scheme 4.1. Proposed photodecomposition mechanism of PVA.

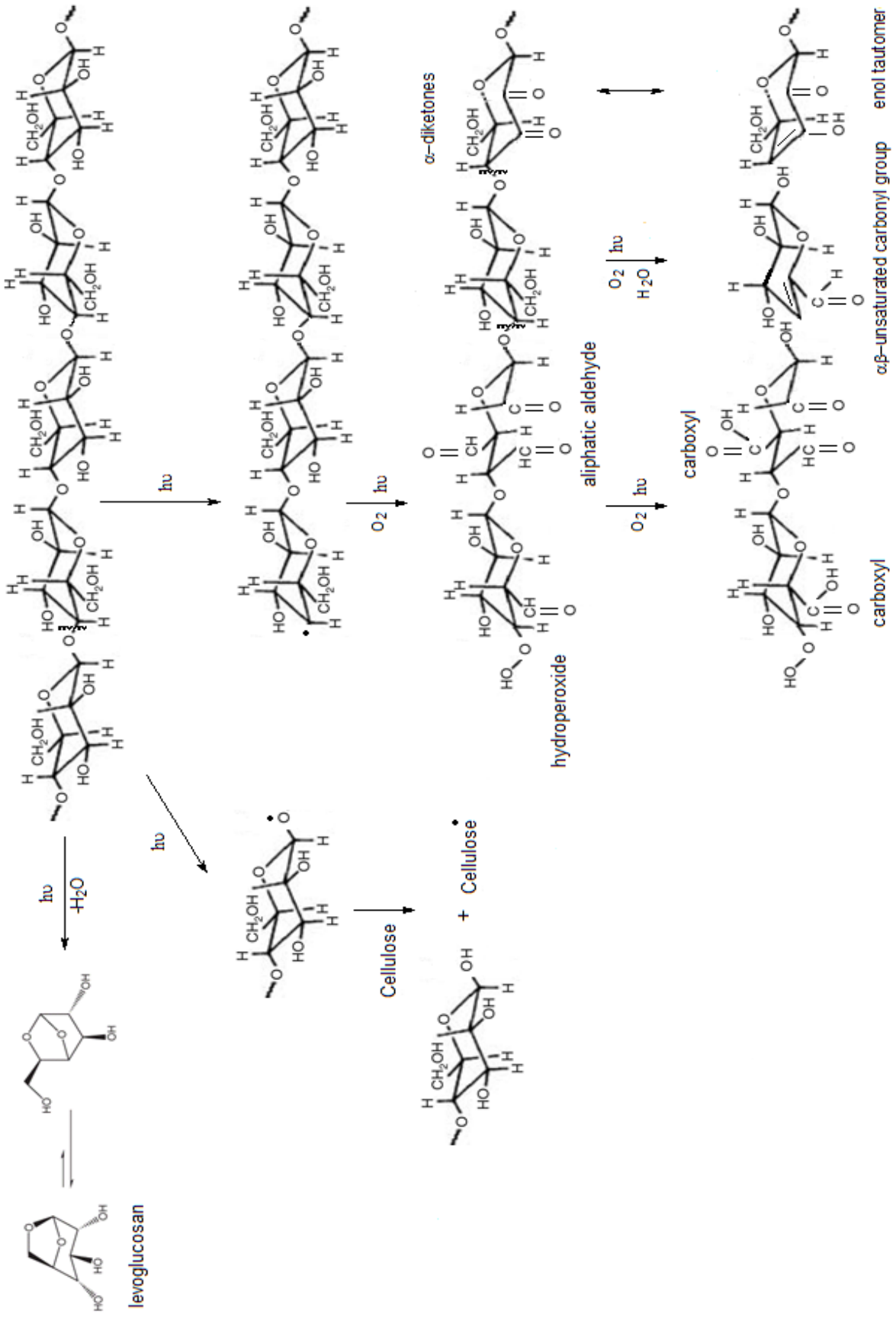

Scheme 4.2. Proposed photodecomposition mechanism of cellulose.

General conclusions

During outdoor expsoure of polymers, environmental factors such as light, heat, UV radiation, oxygen from air and humidity act simultaneously, leading to irreversible structural modifications and thus reducing the efficiency and lifetime of the materials.

For surpassing this impediment, several methods may be applied, such as stabilization or chemical modification of surfaces. In order to select the most appropriate and efficient approach for protection of polymeric materials against weathering, a detailed knowledge of the aspects related to the kinetics and mechanistics of different degradation reactions must be obtained.

Six SIPN stuctures based on aromatic linear PUR and increasing concentrations of CER (5%, 10%, 15%, 20%, 30% and 40%), with their synthesis described in the literature, were characterized in terms of miscibility, thermal stability in inert media (nitrogen) and photochemical stability and the following conclusions could be derived:

- ✓ the SIPNs based on an aromatic PUR and increasing CER content (5%, 10%, 15%, 20%, 30%, 40%) showed a good miscibility up to a CER content of 30%;
- ✓ DSC measurements and microscopy studies (OM, SEM) indicated phase separation for an CER content of 40% in the SIPN structures;
- ✓ there was evidentiated the presence of specific and strong interactions between the networks components;
- ✓ the thermal degradation of the SIPN samples occured in three successive stages;
- ✓ the content of CER in SIPN samples changed the starting temperature of thermal degradation;
- ✓ the thermal decomposition reaction mechanism and the kinetic parameters of each stage depended on CER content;
- ✓ the increase in CER content significantly influenced the rate of thermal degradation;
- ✓ water, ammonia, alcohols, oxygen traces and carbon oxides were identified amongst the gases released during the thermal decomposition of SIPN samples;
- ✓ changes in the surface properties such as colour, gloss and contact angles were investigated during SIPN samplec irradiation;
- ✓ color changes were lesser for SIPN structures than for PUR films, due to their highest transparency, thus beeing deeper penetrated by UV radiation;
- ✓ CER content increase did not seem to significantly affect the variation of gloss retention. Contact angle variation significantly decreased
- ✓ there also exists the possibility of photochemical protection of the polyurethane for the networks containing up to 20% ERN due to films opacity increase due CER's light retention;
- ✓ phase separation occurred for sample SIPN5 which contained more than 20% CER.
- ✓ the mass losses were similar for all samples after UV irradiation.

Cryogels based on poly(vinyl alcohol) and varying cellulose content (10%, 30% and 50%) were exposed to different UV irradiation doses and the following conclusions could be derived:

- ✓ the cryogels showed a discoloration tendency with irradiation dose increase, due to lightness factor and chromatic coefficients values increase;
- ✓ structural modifications during the photodecomposition were monitored by using FTIR, UV–Viz, XPS and TGA–MS techinques;
- ✓ PVA underwent a slower photooxidation process, due to hardening of air diffusion;
- ✓ intermediate hydroperoxide formation which was confirmed by an iodometric method;
- ✓ pure cellulose exhibited photooxidation phenomena in bulk by continuous hydroperoxide formation and depolymerization, because of the gaps between chains;
- ✓ cellulose chains were protected from UV irradiation by a concentration of PVA up to 70%.

Scientific activity

The original research presented in this Ph.D. thesis was detailed in **10 scientific publications**, of which 8 published, 1 accepted and 1 under consideration for publication in international journals, **1 book chapter** accepted for publication at an international publisher, **14 oral communications** and **12 posters** presented at scientific national and international conferences.

- **SCIENTIFIC PUBLICATIONS**

1. **C.–D. Varganici**, A. Durdureanu–Angheluta, D. Rosu, M. Pinteala, B.C. Simionescu, Thermal degradation of magnetite nanoparticles with hyrdrophilic shell. *J. Anal. Appl. Pyrol.* **2012**, *96*, 63–68.
IF = 3.070

2. D. Rosu, L. Rosu, F. Mustata, **C.–D. Varganici**, Effect of UV radiation on some semi–interpenetrating polymer networks based on polyurethane and epoxy resin. *Polym. Degrad. Stab.* **2012**, *97* (8), 1261–1269.
IF = 2.633

3. **C.–D. Varganici**, L. Rosu, D. Rosu, B.C. Simionescu, Miscibility studies of some semi–interpenetrating polymer networks based on an aromatic polyurethane and epoxy resin. *Compos. Part B: Eng.* **2013**, *50*, 273–278.
IF = 2.602

4. D. Rosu, L. Rosu, **C.–D. Varganici**, The thermal stability of some semi–interpenetrated polymer networks based on epoxy resin and aromatic polyurethane. *J. Anal. Appl. Pyrol.* **2013**, *100*, 103–110.
IF = 3.070

5. **C.–D. Varganici**, O. Ursache, C. Gaina, V. Gaina, D. Rosu, B.C. Simionescu, Synthesis and characterization of a new thermoreversible polyurethane network. *Ind. Eng. Chem. Res.* **2013**, *52* (15), 5287–5295.
IF = 2.235

6. M. Aflori, B. Simionescu, I.–E. Bordianu, L. Sacarescu, **C.–D. Varganici**, F. Doroftei, A. Nicolescu, M. Olaru, Silsesquioxane–based hybrid nanocomposites with methacrylate units containing titania and/or silver nanoparticles as antibacterial/antifungal coatings for monumental stones. *Mat. Sci. Eng. B* **2013**, *178* (19), 1339–1346.
IF = 2.122

7. **C.–D. Varganici**, O.M. Păduraru, L. Rosu, D. Rosu, B.C. Simionescu, Thermal stability of some cryogels based on poly(vinyl alcohol) and cellulose, *J. Anal. Appl. Pyrol.* **2013**, *104*, 77–83.
IF = 3.070

8. L. Rosu, D. Rosu, C.–C. Gavat, **C.–D. Varganici**, Photochemical stability of cellulose textile surfaces painted with some reactive azo–triazine dyes. *J. Mater. Sci.* **2014**, *49* (13), 4469–4480.
IF = 2.305

9. **C.–D. Varganici**, L. Rosu, O.M. Mocanu (Paduraru), D. Rosu, Influence of poly(vinyl alcohol) on cellulose photochemical stability in cryogels during UV irradiation. *J. Photochem. Photobiol. A: Chem.* **2014**
DOI: 10.1016/j.jphotochem.2014.10.00
IF = 2.291

10. D. Rosu, R. Bodîrlău, C.–A. Teacă, L. Rosu, **C.–D. Varganici**, FTIR spectroscopy and colour changes of softwood coated with soybean oil and photodegraded under UV light. *Wood Sci. Technol.* **2014** (under consideration).
IF = 1.873

- **ORAL COMMUNICATIONS PRESENTED AT NATIONAL AND INTERNATIONAL SCIENTIFIC CONFERENCES**

1. **C.–D. Varganici**, O. Ursache, C. Gaina, V. Gaina, B.C. Simionescu, DSC studies on thermoreversible and non–thermoreversible hybrid materials, *21st Symposium on Thermal Analysis and Calorimetry*, February 17th, 2012, Romanian Academy, Bucharest (Romania).

2. **C.–D. Varganici**, L. Rosu, M. Pinteala, D. Rosu, B.C. Simionescu, Thermal analysis application to some polymeric material micro– and nanoparticles, *Materials Characterization by Thermal Analysis Techniques* (seminar), "Petru Poni" Institute of Macromolecular Chemistry, May 24th, 2012, Iassy (Romania).

3. O. Ursache, C. Gaina, V. Gaina, **C.–D. Varganici**, Thermoreversible polyurethanes obtained from A3B2 monomers, *Scientific Communication Session for Students, Master's and PhD students – IIIrd Edition*, „Alexandru Ioan Cuza" Univeristy, May 26th, 2012, Iassy (Romania).

4. **C.–D. Varganici**, A. Durdureanu–Angheluta, F. Doroftei, D. Rosu, M. Pinteala, B.C. Simionescu, Core–shell magnetic nanoparticles based on silane compounds and magnetite: Thermal behavior, *Fifth Cristofor I. Simionescu Symposium "Frontiers in Macromolecular and Supramolecular Science"*, Romanian Academy, June 11–13th, 2012, Bucharest (Romania).

5. D. Rosu, L. Rosu, **C.–D. Varganici**, Le comportement photochimique et thermique des systèmes polymérique multicomposant, *Septième Colloque Franco–Roumain de Chimie Appliquée (COFrRoCA)*, "Vasile Alecsandri" University, June 27–29th, 2012, Bacău (Romania).

6. **C.–D. Varganici**, O. Ursache, C. Gaina, V. Gaina, B.C. Simionescu, Nouveau matériaux hybride autorenouvelable thermique. Etudes thermiques, *Septième Colloque Franco–Roumain de Chimie Appliquée (COFrRoCA)*, "Vasile Alecsandri" University, June 27–29th, 2012, Bacău (Romania).

7. O. Ursache, C. Gaina, V. Gaina, N. Tudorachi, **C.–D. Varganici**, E. Buruiana, Nouveaux réseaux thermorevérsibles polyvinyle furfural–polyetheruréthane, *Septième Colloque Franco–Roumain de Chimie Appliquée (COFrRoCA)*, "Vasile Alecsandri" University, June 27–29th, 2012, Bacău (Romania).

8. D. Rosu, **C.–D. Varganici**, L. Rosu, Thermal decomposition study of some polymeric multicomponent systems based on aromatic polyurethane and epoxy resin network, *7th MoDeSt Conference*, September 2–6th, 2012, Prague (Czech Republic).

9. **C.–D. Varganici**, D. Rosu, L. Rosu, The effect of temperature on the thermal stability of some semi–interpenetrated polymer networks based on epoxy resin and aromatic polyurethane, *XXXIInd National Chemistry Conference*, Călimănești–Căciulata, October 3–5th, 2012, Vâlcea (Romania).

10. **C.–D. Varganici**, L. Rosu, D. Rosu, B.C. Simionescu, Semi–interpenetrating polymer networks based on an aromatic polyurethane and epoxy resin. Miscibility studies, *European Polymer Congress (EPF 2013)*, June 16–21th, 2013, Pisa (Italy).

11. **C.–D. Varganici**, D. Rosu, L. Rosu, B.C. Simionescu, Epoxy and polyurethane based S-IPNs as coating materials. Miscibility through thermal studies, *XXIVth Session of Scientific Communications of the „Petru Poni" Institute of Macromolecular Chemistry – Progress în Organic and Macromolecular Compounds (ZAI 2013)*, October 3–5th, 2013, Iassy (Romania).

12. O.–M. Mocanu (Paduraru), **C.–D. Varganici**, L. Rosu, D. Rosu, Thermal decomposition study of poly(vinyl alcohol)/cellulose based cryogels via TG/FTIR–MS analysis, *XXIVth Session of Scientific Communications of the „Petru Poni" Institute of Macromolecular Chemistry – Progress în Organic and Macromolecular Compounds (ZAI 2013)*, October 3–5th, 2013, Iassy (Romania).

13**. C.–D. Varganici**, D. Rosu, O. M. Mocanu (Paduraru), L. Rosu, On the thermal stability of poly(vinyl alcohol) and cellulose based cryogels, *8th MoDeSt Conference*, August 31st–September 4th, 2014, Portorose (Slovenia).

14. D. Rosu, **C.–D. Varganici**, L. Rosu, Accelerated photoaging of dyed textiles, *8th MoDeSt Conference*, August 31st–September 4th, 2014, Portorose (Slovenia).

- **POSTERS**

1. L. Rosu, F. Mustata, D. Rosu, **C.–D. Varganici**, Semi–interpenetrating polymer networks polyurethane–epoxy resin. Study of photochemical stability, *7th MoDeSt Conference*, September 2–6th, 2012, Prague (Czech Republic).

2. **C.–D.Varganici**, A. Durdureanu–Angheluta, D. Rosu, M. Pinteala, B.C. Simionescu, Thermal stability of core–shell hydrophilic nanoparticles for biomedicine, *7th MoDeSt Conference*, September 2–6th, 2012, Prague (Czech Republic).

3. O. Ursache, C. Gaina, V. Gaina, **C.–D.Varganici**, New polyurethane thermoreversible networks, *4th Bilateral Symposium on Functional Heterocyclic and Heterochain Polymers for Advanced Materials*, "Petru Poni" Institute of Macromolecular Chemistry, September 2–7th, 2012, Iassy (Romania).

4. D. Rosu, L. Rosu, **C.–D. Varganici**, Photooxidation behavior of some polyurethane based semi–interpenetrated polymer networks, *XXXIInd National Chemistry Conference*, Călimănești–Căciulata, October 3–5th, 2012, Vâlcea (Romania).

5. C.–A. Teaca, R. Bodirlau, L. Rosu, D. Rosu, **C.–D. Varganici**, Wood treatment with organic anhydride and epoxidized vegetable oil – thermal properties investigation, *XXXIInd National Chemistry Conference*, Călimănești–Căciulata, October 3–5th, 2012, Vâlcea (Romania).

6. D. Rosu, C.–C. Gavat, L. Rosu, **C. –D. Varganici**, Cellulose fabrics painted with some reactive azotriazine dyes. Photochemical behaviour, *European Polymer Congress (EPF 2013)*, June 16–21th, 2013, Pisa (Italy).

7. L. Rosu, **C.–D. Varganici**, D. Rosu, Semi–interpenetrating polymer networks based on an aromatic polyurethane and epoxy resin. Surface properties modifications, *European Polymer Congress (EPF 2013)*, June 16–21th, 2013, Pisa (Italy).

8. F. Mustata, I. Bicu, D. Rosu, **C.–D.Varganici**, Epoxy monomers based on methyl ester of corn oil, *European Polymer Congress (EPF 2013)*, June 16–21th, 2013, Pisa (Italy).

9. **C.–D. Varganici**, A. Coroaba, R. Bodirlau, C.–A. Teaca, L. Rosu, D. Rosu, Studies on Structural and Thermal of chemically modified wood, *XXIVth Session of Scientific Communications of the „Petru Poni" Institute of Macromolecular Chemistry – Progress în Organic and Macromolecular Compounds (ZAI 2013)*, October 3–5th, 2013, Iassy (Romania).

10. R. Bodirlau, C.–A. Teaca, D. Rosu, L. Rosu, **C.–D. Varganici**, Starch/wood bio–based polymer systems – Structure and thermal properties, *8th MoDeSt Conference*, August 31st–September 4th, 2014, Portorose (Slovenia).

11. L. Rosu, **C.–D. Varganici**, O. M. Mocanu (Paduraru), E. Marlica, On the photodegradation of poly(vinyl alcohol) and cellulose based cryogels, *8th MoDeSt Conference*, August 31st–September 4th, 2014, Portorose (Slovenia).

12. F. Mustata, E. Marlica, N. Tudorachi, I. Bicu, **C.–D. Varganici**, Curing reactions of epoxidized methyl esters of corn oil and thermal characterization of the obtained crosslinked products, August 31st–September 4th, 2014, Portorose (Slovenia).

- **BOOK CHAPTER**

1. D. Rosu, **C.–D. Varganici**, L. Rosu, O. M. Paduraru, Thermal degradation of thermosetting blends, în *Thermal Degradation of Polymer Blends, Composites and Nanocomposites*, P.M. Visakh, Y. Arao (Eds.), Springer (accepted for publication), 2014.

- **MEMBER IN RESEARCH PROJECTS**

1. Project PN–II–ID–PCE–2011–3–0187, Advanced researches related to the behavior of multi–component polymer systems under simulated environmental factors action, Coordinator: "Petru Poni" Institute of Macromolecular Chemistry, Iassy; project manager: Dr. Dan Roșu.

2. Project PN–II–RU–TE–2012–3–0123, nr. 28/29.04.2013, Polymers containing phosphor for high performance materials for advanced technologies and/or biomedical applications, Coordinator: "Petru Poni" Institute of Macromolecular Chemistry, Iassy; project manager: Dr. Diana Serbezeanu.

3. European Project Regional Development Fund, Sectoral Operational Programme ''Increase of Economic Competitiveness'', Priority Axis 2 (SOP IEC–A2–O2.1.2–2009–2, ID 570, COD SMIS–CSNR: 12473, Contract 129/2010–POLISILMET); project manager: Dr. Maria Cazacu.

Selective references

73. Rosu, D.; Rosu, L.; Mustata, F.; **Varganici, C.-D.**, Effect of UV radiation on some semi-interpenetrating polymer networks based on polyurethane and epoxy resin. *Polymer Degradation and Stability* 2012, 97, (8), 1261-1269.
74. Ciobanu, C.; Afloarei, P.; Barladeanu, P.; Culic, C. Patent number 93590; 1987.
75. Rosu, L. New mulitcomponent polyurethane based materials. Structure–Morfology–Properties relationships. PhD Thesys, "Gheorghe Asachi" Technical University, Iassy, 2003.
76. Cristea, M.; Ibanescu, S.; Cascaval, C. N.; Rosu, D., Dynamic mechanical analysis of polyurethane–epoxy interpenetrating polymer networks. *High Performance Polymers* 2008, 21, (5), 608-623.
77. Cascaval, C. N.; Ciobanu, C.; Rosu, D.; Rosu, L., Polyurethane-epoxy maleate of bisphenol a semi-interpenetrating polymer networks. *Journal of Applied Polymer Science* 2002, 83, (1), 138-144.
78. Aubin, M.; Bédard, Y.; Morrissette, M.-F.; Prud'homme, R. E., Miscible blends prepared from two crystalline polymers. *Journal of Polymer Science: Polymer Physics Edition* 1983, 21, (2), 233-240.
79. Harrison, I. R.; Runt, J., Incompatible blends: Thermal effects in a model system. *Journal of Polymer Science: Polymer Physics Edition* 1980, 18, (11), 2257-2261.
80. **Varganici, C.-D.**; Rosu, L.; Rosu, D.; Simionescu, B. C., Miscibility studies of some semi-interpenetrating polymer networks based on an aromatic polyurethane and epoxy resin. *Composites Part B: Engineering* 2013, 50, 273-278.
81. Fox, T. G., Influence of diluent and of copolymer composition on the glass temperature of a polymer system. *Bulletin of the American Physical Society* 1956, 1, 123-125.
82. Lu, S.; Pearce, E. M.; Kwei, T. K., Synthesis and characterization of (4-vinylphenyl)dimethylsilanol polymer and copolymers. *Macromolecules* 1993, 26, (14), 3514-3518.
83. Singh, V. B.; Walsh, D. J., The miscibility of polyethersulfone with phenoxy resin. *Journal of Macromolecular Science, Part B* 1986, 25, (1), 65-87.
84. Gordon, M.; Taylor, J. S., Ideal copolymers and the second-order transitions of synthetic rubbers. I. non-crystalline copolymers. *Journal of Applied Chemistry* 1952, 2, (9), 493-500.
93. Rosu, D.; Rosu, L.; **Varganici, C.-D.**, The thermal stability of some semi-interpenetrated polymer networks based on epoxy resin and aromatic polyurethane. *Journal of Analytical and Applied Pyrolysis* 2013, 100, 103-110.
106. Silverstein, R. M.; Webster, F. S.; Kiemle, D. J., *Spectrometric identification of organic compounds.* 7 ed.; John Wiley & Sons: New York, 2005.
114. Paduraru, O. M.; Vasile, C.; Patachia, S.; Grigoras, C.; Oprea, A. M., Membranes based on poly(vinyl alcohol)/b-cyclodextrin blends. *Polymery* 2010, 55, (6), 473-478.
124. **Varganici, C.-D.**; Rosu, L.; Păduraru (Mocanu), O. M.; Rosu, D., Influence of poly(vinyl alcohol) on cellulose photochemical stability in cryogels during UV irradiation. *Journal of Photochemistry and Photobiology A: Chemistry* 2014 (acceptată).
139. Ursache, O.; Gaina, C.; Gaina, V.; Tudorachi, N.; Bargan, A.; Varganici, C.-D.; Rosu, D., Studies on Diels-Alder thermoresponsive networks based on ether-urethane bismaleimide functionalized poly(vinyl alcohol). *Journal of Thermal Analysis and Calorimetry* 2014.
DOI :10.1007/s10973-014-4041-7
140. Rosu, D.; Bodîrlău, R.; Rosu, L.; Teacă, C.-A., **Varganici, C.-D.**, FTIR spectroscopy and colour changes of softwood coated with soybean oil and photodegraded under UV light. *Wood Science and Technology* 2014 (under consideration).

Results presented in this Ph.D. thesis were obtained during the activities conducted in the Project "Advanced researches related to the behavior of multi–component polymer systems under simulated environmental factors action", Project PN–II–ID–PCE–2011–3–0187, Coordinator: "Petru Poni" Institute of Macromolecular Chemistry, Iassy; project manager: Dr. Dan Roșu.